Phys. Status Solidi A **209**, No. 1, 75–78 (2012) / **DOI** 10.1002/pssa.201100148

physica status solidi a
www.pss-a.com
applications and materials science

Band gap reduction and dielectric function of $Ga_{1-x}Zn_xN_{1-x}O_x$ and $In_{1-x}Zn_xN_{1-x}O_x$ alloys

Maofeng Dou[*,1] **and Clas Persson**[1,2]

[1] Department of Materials Science and Engineering, Royal Institute of Technology, 100 44 Stockholm, Sweden
[2] Department of Physics, University of Oslo, PO Box 1048 Blindern, 0316 Oslo, Norway

Received 6 May 2011, revised 29 June 2011, accepted 15 July 2011
Published online 22 November 2011

Keywords absorption, band gap, dielectric function, GaN, InN, semiconductor alloys, ZnO

[*] Corresponding author: e-mail maofeng@kth.se, Phone: +46 8 790 8930, Fax: +46 8 20 7681

The band gap reductions, dielectric functions and absorption coefficients of the $Ga_{1-x}Zn_xN_{1-x}O_x$ and $In_{1-x}Zn_xN_{1-x}O_x$ ($x = 0.00$, 0.25, 0.50, 0.75, and 1.00) alloys were calculated, employing the partial self-consistent GW approximation. As a comparison, the local density approximation (LDA) and the Heyd–Scueria–Ernzerhof (HSE) hybrid functional were also used to calculate the gap reduction. Both $Ga_{1-x}Zn_xN_{1-x}O_x$ and $In_{1-x}Zn_xN_{1-x}O_x$ alloys show strong band gap bowing. As a result, the band gap energy in $Ga_{1-x}Zn_xN_{1-x}O_x$ is reduced by $E_g(GaN) - E_g(Ga_{1-x}Zn_xN_{1-x}O_x) = 1.61$, 2.01 and 1.91 eV for $x = 0.25$, 0.50, and 0.75, respectively. This allows optoelectronic devices based on GaN and ZnO with more efficient absorption or emission of light in the visible light range. The calculated dielectric functions and absorption spectra demonstrate that the band gap reduction enhances the optical absorption around the 2.5 eV region. Interestingly, the $In_{1-x}Zn_xN_{1-x}O_x$ alloy with $x = 0.25$ has the large optical absorption coefficient in the energy region 0.69–6.0 eV, and the alloy has very good absorption at 2–3 eV.

1 Introduction GaN, InN and ZnO are important optoelectronic materials in many application fields. They have the same crystal structure (wurtzite structures at low temperature, $P6_3mc$ space group) and rather similar band gaps: $E_g(GaN) = 3.50$ eV and $E_g(ZnO) = 3.40$ eV [1, 2]. However, recent researches have shown that incorporating one material into the other could significantly reduce the band gap. Maeda et al. [3] reported that randomly incorporating ZnO into GaN host (with 22% ZnO) reduces the optical band gap to 2.60 eV, and randomly incorporating GaN into ZnO host (with 15% GaN) reduces the optical band gap to 2.50 eV [4]. Huda et al. [5] also have shown that this band gaps reduction is not symmetric, that is, incorporating GaN in ZnO host (with 1.85% GaN) reduces the band gap much more than that of incorporating ZnO in GaN host (with 1.85% ZnO) based on theoretical calculation. This kind of compound exhibits visible luminescence [6, 7] and can high efficiently split water under visible light [8–10]. It is also observed that $In_{1-x}Zn_xN_{1-x}O_x$ reduces the band gap significantly compared to that of pure ZnO, and thereby create a new optical absorption band in the long wavelength region [11]. There is however still a lack of growth and characterization of the $In_{1-x}Zn_xN_{1-x}O_x$ alloys.

In this work, we have investigated the band gap reductions, dielectric functions and optical absorptions of $Ga_{1-x}Zn_xN_{1-x}O_x$ and $In_{1-x}Zn_xN_{1-x}O_x$ alloys through partial self-consistent GW approximation (GW). As comparison, the local density approximation (LDA) and the Heyd–Scueria–Ernzerhof (HSE) hybrid functional were also used to calculate the band gaps. Although it is still not clear whether GaN and ZnO form random alloy, cluster structure, or if the compounds are thermodynamic stable, some experimental studies show that random alloys can be synthesized [3, 4]. Also, theoretical simulation have shown that at high temperature random alloy could be formed [12, 13]. We therefore model the $Ga_{1-x}Zn_xN_{1-x}O_x$ and $In_{1-x}Zn_xN_{1-x}O_x$ alloys with a single randomly chosen structure for each concentration.

2 Computational details The calculations were performed using the projector augmented wave (PAW) [14, 15] basis considering the Zn 3d as valence electrons,

whereas the localized Ga 3d and In 4d electrons were treated as core electrons. The plane-wave cutoff energy was set to 370 eV, and the internal cutoff energy in the GW calculation was set to 80 eV based on carefully test. For HSE, the short-range exchange part is described by 25% Hartree–Fock exchange functional and 75% Perdew–Burke–Ernzerhof (PBE) functional. The screening parameter was set to 0.2 $Å^{-1}$ as suggested by Heyd et al. [16, 17].

The supercells were built from $2 \times 2 \times 2$ primitive cells (32 atoms) and fully relaxed (both internal and external parameters) through LDA approach. Brillouin-zone integration was performed with $2 \times 2 \times 2$ Monkhorst–Pack $\boldsymbol{k}$-mesh. $In_{1-x}Zn_xN_{1-x}O_x$ with $x = 0.50$ were calculated with $2 \times 2 \times 1$ supercell and $4 \times 4 \times 4$ Monkhorst–Pack $\boldsymbol{k}$-mesh.

The dielectric function here was calculated within the independent particle picture, and the optical momentum matrix was calculated in the long wavelength $q = |\boldsymbol{k}' - \boldsymbol{k}| = 0$ limit. The imaginary part of the dielectric function reads

$$\varepsilon_2^{\alpha\beta}(\omega) = \frac{4\pi^2 e^2}{\Omega m_e^2 \omega^2} \times \sum_{knn'\sigma} \langle \boldsymbol{k}n\sigma | \boldsymbol{p}_\alpha | \boldsymbol{k}n'\sigma \rangle \langle \boldsymbol{k}n'\sigma | \boldsymbol{p}_\beta | \boldsymbol{k}n\sigma \rangle \times f_{\boldsymbol{k}n\sigma}(1 - f_{\boldsymbol{k}n'\sigma}) \delta(E_{n'\sigma}(\boldsymbol{k}) - E_{n\sigma}(\boldsymbol{k}) - \hbar\omega), \quad (1)$$

where e is the electron charge, $\boldsymbol{p}$ the momentum operator, Ω the crystal volume, m_e the electron static mass, $f_{\boldsymbol{k}n\sigma}$ the Fermi distribution and $|\boldsymbol{k}n\sigma\rangle$ is the crystal wave function corresponding to the n-th eigenvalue $E_{n\sigma}(\boldsymbol{k})$ with crystal momentum $\boldsymbol{k}$ and spin σ. The delta Dirac function indicates the importance of describing the band gap correctly. The real part of the dielectric function is obtained from the Kramers–Kronig dispersion transformation [18].

3 Result and discussion From the GW calculation we analyse the optical properties of $Ga_{1-x}Zn_xN_{1-x}O_x$ and $In_{1-x}Zn_xN_{1-x}O_x$ in terms of the band gap energy $E_g(x)$, the complex dielectric function $\varepsilon(\omega) = \varepsilon_1(\omega) + i\varepsilon_2(\omega)$ and the absorption coefficient $\alpha(\omega)$ as functions of the ZnO content x.

3.1 Band gap The GW calculations show that $Ga_{1-x}Zn_xN_{1-x}O_x$ and $In_{1-x}Zn_xN_{1-x}O_x$ alloys have direct band gaps at the Γ-point which were listed in Table 1, LDA and HSE band gaps were also listed for comparison. The LDA underestimates the band gaps of both GaN and ZnO. As expected, HSE improved the GaN band gap considerably, but HSE still underestimated the ZnO band gap (only 2.58 eV).

This underestimate is mainly due to that HSE overestimate the energetic position of the Zn 3d, locating the states ~5.4 eV below the valence band maximum. By applying the quasi-particle correction within the GW approximation, the generated band gaps of both GaN and ZnO are quite close to the experimental values. Also the energy position of the Zn 3d is improved to ~6.9 eV below valence band maximum which is close to the experimental data of ~7.0 eV [19].

Table 1 The calculated fundamental band gap E_g of $Ga_{1-x}Zn_xN_{1-x}O_x$ and $In_{1-x}Zn_xN_{1-x}O_x$ alloys with $x = 0.00$, 0.25, 0.50, 0.75 and 1.00. The E_g refers to the direct Γ-point gap and in the unit of eV.

	ZnO content x				
	0.00	0.25	0.50	0.75	1.00
$Ga_{1-x}Zn_x N_{1-x}O_x$					
LDA	2.03	0.59	0.12	0.20	0.80
HSE	3.41	1.83	1.45	1.61	2.58
GW	3.67	2.06	1.66	1.76	3.10
$In_{1-x}Zn_xN_{1-x}O_x$					
LDA	0.00	0.03	0.12	0.25	0.80
HSE	0.69	0.85	1.12	1.60	2.58
GW	0.51	0.69	1.26	1.83	3.10

When GaN alloyed with 25% of ZnO (*i.e.*, $x = 0.25$), the band gap is significantly reduced. When alloyed with 50% ZnO ($x = 0.50$) the band gap is further reduced to 1.66 eV, and further incorporating ZnO increase the band gaps. The top valence bands of GaN are constituted by N p-like state. The Ga d-like states are deeply below the N p-like state. However, in ZnO, the Zn d-like states are near the top of valence bands. When Ga and N were substituted by Zn and O, respectively, the top valence bands are constituted by anion (N and O) p-like states and the cation (Zn) d-like states. The bottom conduction bands are constituted by cation (Ga and Zn) s–p hybridized state (Fig. 1). The possible reason for the band gap reduction might be: when alloyed with ZnO, O and Zn replaced the N and Ga site, respectively, the repulsion between Zn-3d state and N-2p state in the valence bands pushes the top valence bands up. Meanwhile, the bottom of conduction bands down shift due to the interaction between O and Ga. This effect is thus different from anion alloying of ZnO with ZnS, where the gap reduction is directly related to the valence- and conduction-band off sets [20].

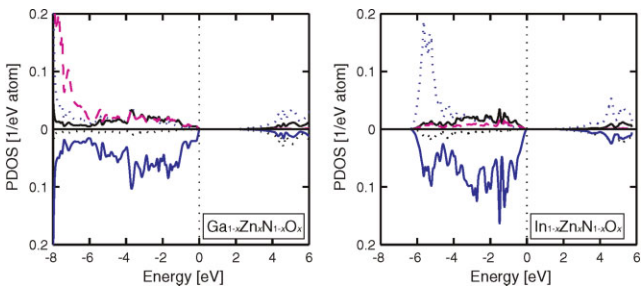

Figure 1 (online colour at: www.pss-a.com) Atom and angular resolved density of state (PDOS) near the band edges of $Ga_{1-x}Zn_xN_{1-x}O_x$ and $In_{1-x}Zn_xN_{1-x}O_x$ alloys with $x = 0.5$ using the GW approach and including a 0.03 eV Lorentzian broadening. The PDOS has been scaled by $(2l+1)^{-1}$ for better visibility. For better visibility, the cation (Zn and Ga) s states (blue dotted), p states (black solid) and d states (magenta dashed) as well as anion (N and O) s states (black dotted) and p states (blue solid) are plotted.

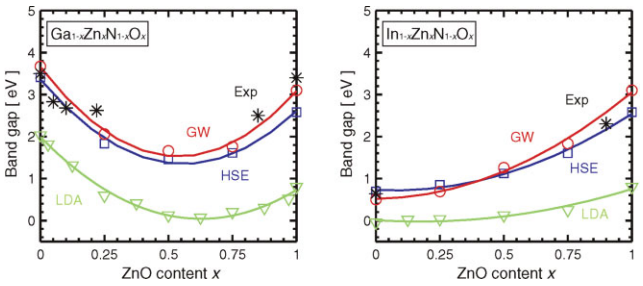

Figure 2 (online colour at: www.pss-a.com) Calculated band gap bowing of $Ga_{1-x}Zn_xN_{1-x}O_x$ and $In_{1-x}Zn_xN_{1-x}O_x$ alloys with $x = 0.00$, 0.25, 0.50, 0.75 and 1.00 through LDA, HSE and GW approaches. The curves were fitted by equation $E_g(x) = (1-x)E_g(A) + xE_g(ZnO) - bx(1-x)$ with A = GaN or InN.

As shown in Fig. 2, the $Ga_{1-x}Zn_xN_{1-x}O_x$ alloys have a strong band gap bowing. The bowing parameter b for the alloys is expressed as $E_g(x) = (1-x)E_g(GaN) + xE_g(ZnO) - bx(1-x)$ [21], where x is the content of ZnO in $Ga_{1-x}Zn_xN_{1-x}O_x$ alloys, $E_g(x)$, $E_g(GaN)$ and $E_g(ZnO)$ are the band gaps of $Ga_{1-x}Zn_xN_{1-x}O_x$ alloys, GaN and ZnO, respectively. The bowing parameters b of LDA, HSE and GW are 4.95, 6.45 and 7.31 eV, respectively. The band gaps fitted from these parameters are somewhat smaller than the experimental values. For instance, the experimental band gaps of 22% ZnO in GaN host and 15% GaN in ZnO host are about 2.68 and 2.50 eV, respectively [3, 4], whereas the GW gave band gaps about 2.29 and 2.25 eV. This can be used to estimate the general trends in the band gaps reduction, as well as to help designing the proper alloy composition.

For $In_{1-x}Zn_xN_{1-x}O_x$, LDA produces an almost zero band gap for InN, whereas HSE and GW approaches generate the band gaps of InN about 0.69 and 0.51 eV, respectively. When alloyed with ZnO, the band gap will increase with increasing the ZnO content x. The $In_{1-x}Zn_xN_{1-x}O_x$ alloy also shows a strong band gap bowing as shown in Fig. 2. The bowing parameters b of HSE and GW are about 2.11 and 2.47 eV, respectively.

3.2 Dielectric function Figure 3 shows the averaged dielectric function of $Ga_{1-x}Zn_xN_{1-x}O_x$ and $In_{1-x}Zn_xN_{1-x}O_x$ alloys. For $Ga_{1-x}Zn_xN_{1-x}O_x$ alloys, the absorption edge red shift due to the reduction of the band gaps. The band edge absorption belongs to the electrons transition from anion (N and O) p-like state in top of valence bands to the cation (Ga and Zn) s–p hybridized state in bottom of conduction bands. Experimental data show a sharp onset in the imaginary part of GaN and an absorption peak below the band gap of ZnO, which comes from the electron–hole interactions; we will discuss the exciton effects of these alloys in a coming work [22]. The absorption intensities of the imaginary dielectric function in the low energy range (from band gap energy to about 2.5 eV for GaN and 5.0 eV for ZnO) are somewhat smaller than that of previous calculation values. This is because our optical property calculation uses fewer $\boldsymbol{k}$-points. Test calculation

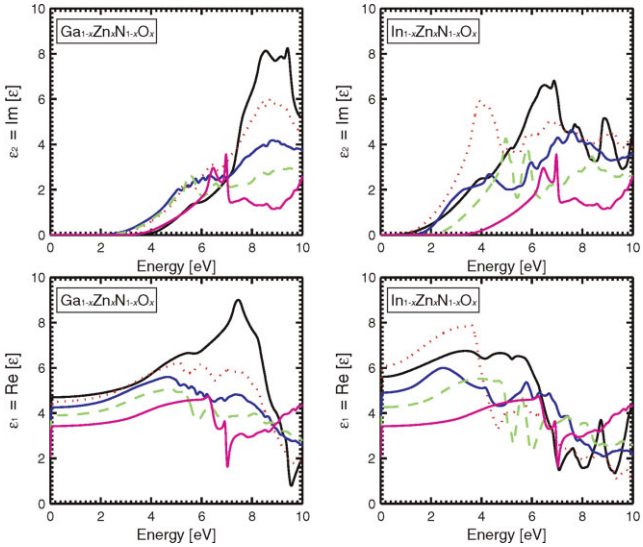

Figure 3 (online colour at: www.pss-a.com) The dielectric function $\varepsilon(\omega) = \varepsilon_1(\omega) + i\varepsilon_2(\omega)$ of $Ga_{1-x}Zn_xN_{1-x}O_x$ and $In_{1-x}Zn_xN_{1-x}O_x$ alloys with $x = 0.00$ (black solid), 0.25 (red dotted), 0.50 (blue solid), 0.75 (green dashed) and 1.00 (magenta solid). A 0.03 eV Lorentzian broadening was used.

with larger number of $\boldsymbol{k}$-points has shown an improvement of the spectra edge, but the overall shape (both position and intensity) of the dielectric function is reliable also for the smaller $\boldsymbol{k}$-mesh. For $In_{1-x}Zn_xN_{1-x}O_x$ alloys, the weak intensity in imaginary dielectric function of InN below 4.0 eV belongs to the transition from top three valence bands to the lowest conduction band. When alloyed with 25% ZnO, the intensity of ε_2 from band edge to ~5.0 eV increased significantly compared with that of InN and ZnO. With further increase of ZnO content x, the absorption decreases gradually. The corresponding dielectric constant ε_∞ of $In_{1-x}Zn_xN_{1-x}O_x$ alloys with $x = 0.25$ is also larger than that of other alloys (as shown in Table 2, $\varepsilon_\infty = 5.60$, 6.08, 4.90, 4.26 and 3.43 with $x = 0.00$, 0.25, 0.50, 0.75 and 1.00, respectively).

Figure 4 shows the optical absorption coefficients of $Ga_{1-x}Zn_xN_{1-x}O_x$ and $In_{1-x}Zn_xN_{1-x}O_x$ alloys. The absorption edges of the alloys red shift due to the reduction of the band gaps. The optical absorption coefficient from band gap edge to ~6.0 eV is slightly larger than that of GaN and ZnO, which is mainly due to the flatter band structure of $Ga_{1-x}Zn_xN_{1-x}O_x$ in the top valence bands and bottom conduction bands. For $In_{1-x}Zn_xN_{1-x}O_x$ alloys, the

Table 2 The high frequency dielectric functions ε_∞ of the alloys for $x = 0.00$, 0.25, 0.50, 0.75 and 1.00 calculated through GW approach. The electron–phonon coupling was excluded.

	ZnO content x				
	0.00	0.25	0.50	0.75	1.00
$Ga_{1-x}Zn_xN_{1-x}O_x$	4.70	4.50	4.27	3.77	3.43
$In_{1-x}Zn_xN_{1-x}O_x$	5.60	6.08	4.90	4.26	3.43

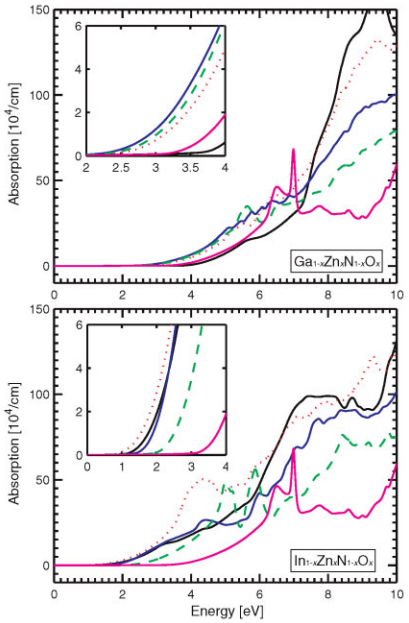

Figure 4 (online colour at: www.pss-a.com) The optical absorption $\alpha(\omega) = (\omega/c) \times [2|\varepsilon(\omega)| - 2\varepsilon_1(\omega)]^{1/2}$ $Ga_{1-x}Zn_xN_{1-x}O_x$ and $In_{1-x}Zn_xN_{1-x}O_x$ alloys with $x = = 0.00$ (black solid), 0.25 (red dotted), 0.50 (blue solid), 0.75 (green dashed) and 1.00 (magenta solid), determined directly from the dielectric function in Fig. 3. The figures inserted are the absorptions at band gap edge. A 0.03 eV Lorentzian broadening was used.

absorption edges increased with increasing of ZnO content x due to the increase of band gaps. The optical absorption coefficient for $x = 0.25$ in the low energy range (from ~0.69 to 6.0 eV) is remarkably larger than that of InN, ZnO and other alloys. This demonstrates that $In_{1-x}Zn_xN_{1-x}O_x$ alloys with low ZnO contents might be a better absorber material in visible and ultraviolet spectrum ranges.

4 Conclusions We have investigated the electronic structures and band gap bowing of $Ga_{1-x}Zn_xN_{1-x}O_x$ and $In_{1-x}Zn_xN_{1-x}O_x$ alloys by LDA, HSE and GW approaches. $Ga_{1-x}Zn_xN_{1-x}O_x$ alloys can reduce the band gaps significantly compared to that of pure GaN and ZnO. The band gaps of $In_{1-x}Zn_xN_{1-x}O_x$ increase gradually with increasing the ZnO content x. Both $Ga_{1-x}Zn_xN_{1-x}O_x$ and $In_{1-x}Zn_xN_{1-x}O_x$ alloys show strong band gap bowing. Our calculations yield band bowing coefficients of $b = 7.31$ and 2.47 eV for $Ga_{1-x}Zn_xN_{1-x}O_x$ and $In_{1-x}Zn_xN_{1-x}O_x$, respectively. The dielectric functions and absorption spectra show that this band gap reduction favours the optical absorption in visible light range. The $In_{1-x}Zn_xN_{1-x}O_x$ alloy with $x = 0.25$ has a larger optical absorption coefficient in the energy range from 0.69 to 6.0 eV.

Acknowledgements This work is supported by the China Scholarship Council, the Swedish Energy Agency and the Swedish Research Council. We acknowledge high-performance computer resources at NSC and HPC2N through SNIC/SNAC.

References

[1] O. Madelung (ed.), Semiconductor-basic Data, 2nd revised ed. (Springer, Berlin, 1996).
[2] J. Wu, W. Walukiewicz, K. M. Yu, J. W. Ager, E. E. Haller, H. Lu, W. J. Schaff, Y. Saito, and Y. Nanishi, Appl. Phys. Lett. **80**, 3967 (2002).
[3] K. Maeda, K. Teramura, T. Takata, M. Hara, N. Saito, K. Toda, Y. Inoue, H. Kobayashi, and K. Domen, J. Phys. Chem. B **109**, 20504 (2005).
[4] M. Mapa, K. S. Thushara, B. Saha, P. Chakraborty, C. M. Janet, R. P. Viswanath, C. Madhavan Nair, K. V. G. K. Murty, and C. S. Gopinath, Chem. Mater. **21**, 2973 (2009).
[5] M. N. Huda, Y. Yan, S. H. Wei, and M. M. Al-Jassim, Phys. Rev. B **78**, 195204 (2008).
[6] T. Hirai, K. Maeda, M. Yoshida, J. Kubota, S. Ikeda, M. Matsumura, and K. Domen, J. Phys. Chem. C **111**, 18853 (2007).
[7] Y. C. Lee, T. Y. Lin, C. W. Wu, H. Teng, C. C. Hu, S. Y. Hu, and M. D. Yang, J. Appl. Phys. **109**, 073506 (2011).
[8] K. Maeda, T. Takata, M. Hara, N. Saito, Y. Inoue, H. Kobayashi, and K. Domen, J. Am. Chem. Soc. **127**, 8286 (2005).
[9] K. Maeda and K. Teramura, Nature **440**, 295 (2006).
[10] M. Yoshida, T. Hirai, K. Maeda, N. Saito, J. Kubota, H. Kobayashi, Y. Inoue, and K. Domen, J. Phys. Chem. C **114**, 15510 (2010).
[11] M. Mapa, K. Sivaranjani, D. S. Bhange, B. Saha, P. Chakraborty, A. K. Viswanath, and C. S. Gopinath, Chem. Mater. **22**, 565 (2010).
[12] S. Z. Wang and L. W. Wang, Phys. Rev. Lett. **104**, 065501 (2010).
[13] L. Li, J. T. Muckerman, M. S. Hybertsen, and P. B. Allen, Phys. Rev. B **83**, 134202 (2011).
[14] G. Kresse and J. Hafner, Phys. Rev. B **47**, 558 (1993).
[15] G. Kresse and J. Joubert, Phys. Rev. B **59**, 1758 (1999).
[16] J. Heyd, G. E. Scuseria, and M. Ernzerhof, J. Chem. Phys. **118**, 8207 (2003).
[17] J. Heyd, G. E. Scuseria, and M. Ernzerhof, J. Chem. Phys. **124**, 219906 (2006).
[18] M. Gajdoš, K. Hummer, G. Kresse, J. Furthmüller, and F. Bechstedt, Phys. Rev. B **73**, 045112 (2006).
[19] C. Persson, C. L. Dong, L. Vayssieres, A. Augustsson, T. Schmitt, M. Mattesini, R. Ahuja, J. Nordgren, C. L. Chang, A. Ferreira da Silva, and J.-H. Guo, Microelectron. J. **37**, 686 (2006).
[20] C. Persson, C. Platzer-Björkman, J. Malmström, T. Törndahl, and M. Edoff, Phys. Rev. Lett. **97**, 146403 (2006).
[21] S. H. Wei and A. Zunger, Phys. Rev. Lett. **76**, 664 (1996).
[22] M. Dou, G. Baldissera, and C. Persson, J. Cryst. Growth, accepted.

